AI-Based Defect Identification in FDM-Printed Biodegradable Polymer Composites Through Multimodal Characterization

Raja Subramani[1,*], K.Ch. Sekhar[2], Jaiprakash Narain Dwivedi[3], V. Venkateswarlu[4], Ramamohana Reddy Maddike[4] and Avvaru Praveen Kumar[5,*]

[1]*Center for Advanced Multidisciplinary Research and Innovation, Chennai Institute of Technology, Chennai, Tamilnadu, India-600069*

[2]*Department of Mechanical Engineering Lendi Institute of Engineering and Technology, Jonnada, Vizianagaram Andhra Pradesh, India-535005*

[3]*Department of Information Technology, Parul Institute of Engineering and Technology, Faculty of Engineering and Technology, Parul University, Vadodara, Gujarat, India*

[4]*Department of Chemistry, Sri Krishnadevaraya University, Anantapur 515003, Andhra Pradesh, India*

[5]*Department of Chemistry, Graphic Era (Deemed to be University), Dehradun-248002, Uttarakhand, India*

Abstract: The growing demand for biodegradable polymer composites in sustainable manufacturing requires robust quality-assessment frameworks that ensure structural reliability and functional performance. However, FDM-based additive manufacturing of such materials often introduces processing-induced defects that compromise mechanical integrity. Conventional visual inspection remains subjective and limited, creating a need for advanced, automated defect-identification strategies. This study addresses this challenge by integrating artificial intelligence with multimodal characterization to establish a reliable defect-detection pipeline for FDM-printed biodegradable polymer composites. Biodegradable PLA-based composites reinforced with microscale and nanoscale fillers were fabricated under controlled FDM conditions, followed by systematic defect mapping through optical imaging, SEM, and surface profilometry. A convolutional neural-network classifier was trained using 2,500 labelled images, incorporating multimodal inputs to identify four major defects: voids, layer gaps, surface roughness irregularities, and under-extrusion patterns. The optimized AI model achieved an overall classification accuracy of 96.4%, precision of 94.8%, recall of 95.3%, and an F1-score of 95.0%, outperforming traditional threshold-based and handcrafted-feature methods. Multimodal correlation analysis further revealed that defects predicted with high probability aligned strongly with SEM-verified structural anomalies (R^2 = 0.93) and surface-roughness deviations (up to 18% variation). These results demonstrate that AI-assisted evaluation offers a reliable, scalable, and non-destructive pathway to improve defect quantification in biodegradable polymer composites. The proposed framework enhances process monitoring, reduces inspection subjectivity, and provides new insights into structure–processing–defect interrelationships in FDM-printed sustainable composites.

Keywords: FDM, Biodegradable polymer composites, Defect identification, Multimodal characterization, Convolutional neural network, Surface analysis, Additive manufacturing.

1. INTRODUCTION

Additive manufacturing (AM), particularly fused deposition modeling (FDM), has emerged as one of the most accessible and versatile fabrication routes for producing polymer-based components across engineering, biomedical, and consumer product domains. As global emphasis on sustainability accelerates, biodegradable polymers such as polylactic acid (PLA), polyhydroxyalkanoates (PHA), and starch-based composites are increasingly deployed as eco-friendly alternatives to conventional petrochemical plastics [1-3]. Their compatibility with composite reinforcement strategies—using natural fibers, nanoscale fillers, or bio-derived particulates—further enhances their appeal in structural and functional applications where improved stiffness, thermal stability, and surface performance are required. Despite these advantages, FDM-printed biodegradable polymer composites are inherently susceptible to process-induced defects originating from thermal gradients, filament flow instabilities, layer-wise deposition inconsistencies, and filler–matrix interactions. Such defects, including voids, interlayer delamination, inadequate layer bonding, under-extrusion bands, and microstructural discontinuities, significantly compromise the mechanical, thermal, and functional properties of the final printed component [4-6]. The challenge becomes more critical in biodegradable systems where material rheology, crystallization behavior, and thermal sensitivity intensify the likelihood of manufacturing defects, making reliable quality monitoring a pressing requirement [7-9]. Existing quality-inspection strategies for FDM predominantly rely on visual inspection, manual assessment, or post-processing destructive testing, all of which are time-consuming, subjective, and unsuitable for rapid or large-scale production.

*Address correspondence to this author Raja Subramani, at the Center for Advanced Multidisciplinary Research and Innovation, Chennai Institute of Technology, Chennai, Tamilnadu, India-600069. E-mail: sraja@citchennai.net; and the author, Avvaru Praveen Kumar, at the Department of Chemistry, Graphic Era (Deemed to be University), Dehradun-248002, Uttarakhand, India. Email: drkumar.kr@gmail.com

Received on 09-11-2025 Accepted on 24-12-2025 Published on 30-12-2025

E-ISSN: 2311-8717/25

Recent advancements in multimodal characterization—such as scanning electron microscopy (SEM), surface profilometry, thermal analysis, and digital optical imaging—have improved the ability to quantify process-related defects, yet these approaches remain limited when performed manually and lack real-time decision-making capability [10-12]. Parallel to these developments, artificial intelligence (AI), particularly deep learning, has shown promise in interpreting complex visual and structural information in manufacturing environments. Recent AI-driven defect-identification studies in additive manufacturing have primarily focused on metallic systems or conventional petroleum-based polymers, often utilizing single-modality inputs such as optical images or thermal signals for defect detection. While convolutional neural networks and machine-learning classifiers have demonstrated promising accuracy in identifying surface anomalies, nozzle clogging, or dimensional deviations, most existing approaches remain limited in their ability to capture microstructural defects or correlate AI predictions with experimentally verified material characteristics. In the context of polymer additive manufacturing, particularly for biodegradable composites, reported studies typically address isolated defect types or rely on handcrafted features, restricting both scalability and interpretability. In contrast, the present study advances beyond incremental visual classification by integrating multimodal characterization combining optical imaging, SEM micrographs, and surface profilometry to enable defect identification across multiple length scales. Furthermore, the proposed framework is specifically tailored to biodegradable polymer composites, a material class that remains underrepresented in AI-based defect-analysis literature despite its growing relevance in sustainable manufacturing.

Convolutional neural networks (CNNs) and transformer-based architectures have revolutionized automated defect detection in metallic AM, injection molding, composites inspection, and non-destructive evaluation. In polymer additive manufacturing, emerging studies have explored AI for layer shifting, Nozzle clogging, and dimensional deviation detection. However, these works are still preliminary, often restricted to single-sensor inputs, limited defect categories, or non-biodegradable materials. Comprehensive AI-driven defect identification frameworks specifically tailored for biodegradable polymer composites are largely absent in the literature [13-15]. Moreover, few studies integrate multimodal data sources—combining optical images, microstructural analyses, and surface-texture data—to improve defect classification accuracy and establish statistical correlations with actual material behavior [16-18]. This gap reveals a critical need for a unified methodology that couples experimental characterization of biodegradable composite prints with advanced AI-based analytics. Addressing this need, the present study proposes an AI-enhanced defect-identification framework for FDM-printed biodegradable polymer composites using multimodal characterization inputs. Biodegradable composite filaments incorporating microscale and nanoscale reinforcements were fabricated and printed under controlled process conditions to generate a diverse dataset of defect scenarios. High-resolution optical images, SEM micrographs, and surface-profilometry data were collected and annotated to create a multimodal training dataset capturing four predominant defect types: voids, interlayer gaps, irregular surface roughness, and under-extrusion patterns. A deep-learning model based on a customized convolutional neural-network architecture was developed to classify these defects, leveraging feature fusion techniques that integrate signals from both macro-scale and micro-scale imaging modalities. The objective of the study is to establish a reliable, automated, and scalable defect-identification methodology that eliminates subjectivity in inspection, accelerates quality assessment, and provides deeper insight into structure–processing–defect relationships in biodegradable polymer composites. Accordingly, the contribution of this work extends beyond incremental algorithmic application by addressing three critical gaps in current research: (i) the development of a multimodal defect database specifically for FDM-printed biodegradable polymer composites, capturing both surface-level and microstructural anomalies; (ii) the implementation of a feature-fusion deep-learning framework that leverages complementary information from optical, SEM, and profilometry data rather than relying on single-sensor inputs; and (iii) the establishment of quantitative correlations between AI-predicted defect severity and experimentally measured surface roughness, void density, and mechanical property degradation. These aspects collectively distinguish the proposed methodology from recent AI-based defect-identification studies that primarily emphasize classification accuracy without experimental validation or materials-specific relevance. Unlike previous studies limited to single-sensor visual data or non-biodegradable materials, this work integrates multimodal information to improve defect-classification robustness and establish mechanistic relationships between filler dispersion, printing conditions, and defect manifestation. By bridging the gap between experimental composite characterization and AI-driven evaluation, this research contributes both a methodological advancement and a practical inspection tool that can support scalable adoption of biodegradable polymer composites in FDM-based production. The remainder of this

manuscript is structured as follows: Section 2 describes the materials, composite preparation, printing parameters, and multimodal characterization techniques employed to generate defect datasets. Section 3 interprets these results in the context of process–structure–property interactions and highlights implications for sustainable composite manufacturing. Finally, Section 4 summarizes the key findings, emphasizes contributions to biodegradable composite quality assurance, and outlines future research directions including real-time monitoring integration and digital-twin development.

2. MATERIALS AND METHODS

Biodegradable polymer composites were developed using polylactic acid (PLA) as the primary matrix material due to its excellent printability, low melting temperature, renewable origin, and widespread utilization in biodegradable applications, making it a suitable model system for defect-identification studies. Polylactic acid (PLA) was selected as the primary matrix material due to its widespread use in fused deposition modeling, stable melt-flow behavior, low processing temperature, and renewable origin, making it a representative biodegradable polymer for defect-identification studies. PLA exhibits predictable rheological and thermal characteristics during extrusion, which is essential for reproducible defect induction and AI-based learning. Micro-calcium carbonate and nanosilica were chosen as reinforcing fillers to intentionally modify melt viscosity, interlayer adhesion, and solidification behavior at different length scales. Microscale $CaCO_3$ was selected to promote flow resistance and localized agglomeration effects, while nanosilica was employed to enhance filler dispersion and interfacial interactions. The selected filler loadings (5 wt% for micro-$CaCO_3$ and 3 wt% for nanosilica) were based on prior literature and preliminary trials indicating stable extrusion behavior, minimal nozzle clogging, and sufficient microstructural variation for defect analysis. To enhance structural features and generate measurable variations in print morphology, two fillers—micro-calcium carbonate and nanosilica—were chosen as environmentally compatible reinforcements with proven ability to modify flow characteristics and interlayer adhesion. The composite synthesis was conducted using a Thermo Scientific HAAKE Rheomex CTW twin-screw micro-compounder, which ensured uniform dispersion of fillers under controlled shear. Before compounding, all materials were dried at 60 °C for 6 h in a Memmert UN75 hot-air oven to avoid moisture-induced void formation. PLA pellets and fillers were fed at predetermined weight ratios (95:5 for microscale and 97:3 for nanoscale composites) selected based on literature indicating stable rheology and minimal nozzle clogging below 5 wt% loading. Melt compounding was performed at 190 °C, 80 rpm for 10 min, producing homogenized composite strands. These strands were subsequently pelletized using a Filabot Pelletizer and extruded into 1.75 mm filaments using a 3Devo Composer Filament Extruder operated at a four-zone temperature profile (175–180–185–190 °C). This profile was selected after preliminary trials showed optimal filament roundness deviation below ±0.05 mm and stable melt flow, which is critical for reproducible FDM printing and controlled defect generation. Filaments were stored in airtight desiccators until printing to prevent humidity-induced swelling.

Sample fabrication was performed using a Bambu Lab A1 FDM printer due to its open-material capability, consistent deposition behavior, and precise process-parameter control. Standard rectangular specimens (100 mm × 20 mm × 4 mm) were printed for mechanical and morphological evaluation, while 20 mm × 20 mm square samples were produced specifically for AI-based defect-image acquisition. These geometries were selected to satisfy ASTM testing requirements and to provide sufficient flat surface area for defect imaging. The melt-compounding temperature of 190 °C and screw speed of 80 rpm were selected to ensure complete polymer melting while preventing thermal degradation of PLA. The four-zone filament extrusion temperature profile (175–180–185–190 °C) was optimized through preliminary trials to achieve uniform filament diameter, low ovality (±0.05 mm), and stable melt flow, which are critical for consistent FDM deposition. These parameters were intentionally chosen to balance print stability with sensitivity to process-induced defect formation, ensuring reliable dataset generation for AI training. The FDM printing parameters were selected to represent commonly adopted industrial and laboratory printing conditions while enabling controlled defect manifestation. A nozzle temperature of 205 °C was chosen to ensure sufficient interlayer diffusion without excessive polymer degradation, whereas a bed temperature of 60 °C promoted adhesion and minimized warping. A layer height of 0.2 mm and nozzle diameter of 0.4 mm were selected to provide adequate resolution for defect visualization while maintaining print stability. The printing speed of 50 mm/s served as a baseline condition, with intentional variations in speed (40–70 mm/s), extrusion multiplier (±10%), and cooling fan speed (0–100%) introduced to generate a diverse range of defect scenarios relevant for AI-based classification and reproducibility. A nozzle temperature of 205 °C was used, as it represents the median temperature achieving balanced surface quality without excessive polymer degradation, while a bed temperature of 60 °C was set to enhance first-layer

adhesion. A printing speed of 50 mm/s was chosen as it provided a stable extrusion rate while allowing the intentional formation of defects when flow inconsistencies occurred. The layer height was fixed at 0.2 mm, a commonly used resolution that ensures adequate layer-boundary visualization for defect identification. The infill density was held constant at 100% to ensure that observed voids or layer gaps resulted from process deviations rather than internal geometry. The nozzle diameter of 0.4 mm was selected because it provides a good balance between detail visibility and ease of defect inspection. To intentionally include controlled variations, additional prints were manufactured by altering extrusion multiplier (±10%), cooling fan speed (0–100%), and print speed (40–70 mm/s) to generate defect-rich datasets while maintaining a baseline reference group.

For morphological assessment, optical imaging was performed using a Leica S9D stereo microscope under uniform LED illumination, capturing high-resolution images for labeling and AI model training. Surface topology was measured using a Mitutoyo SJ-210 surface roughness tester, operated according to ISO 4287 standards, providing quantitative Ra and Rz values for correlation with predicted defects. Microstructural analysis was conducted using a JEOL JSM-IT200 SEM operated at 15 kV, enabling visualization of interlayer bonding, void presence, filler dispersion, and micro-crack propagation. Samples for SEM were cryogenically fractured using liquid nitrogen to preserve fracture morphology and sputter-coated with a 10 nm gold layer using a Quorum Q150R coater to reduce charge accumulation.

Mechanical testing was performed in compliance with ASTM D638 Type V for tensile specimens and ASTM D790 for flexural characterization, using an Instron 3369 universal testing machine with a 5 kN load cell. These standards were selected because they are widely used for polymer composites and allow direct correlation between mechanical degradation and defect severity. For thermal evaluation, differential scanning calorimetry (DSC) and thermogravimetric analysis (TGA) were performed using a TA Instruments SDT Q600, providing insights into composite thermal stability and crystallization behavior, which influence defect formation during printing. These characterization techniques were chosen due to their complementary ability to quantify both macro-scale and micro-scale defect parameters.

All images were labeled manually by three independent evaluators to create a reliable ground-truth dataset for AI training, covering four primary defect categories: voids, layer gaps, roughness irregularities, and under-extrusion patterns. This classification strategy was selected after evaluating the most frequently occurring FDM defects and their direct influence on structural and surface properties. The multimodal dataset (optical, SEM, and profilometry) enabled high-fidelity representation of defects across scales, serving as a crucial justification for integrating diverse inputs within the AI model. The entire materials-and-methods framework was designed to ensure controlled composite synthesis, reproducible printing, intentional defect generation, and rigorous characterization—providing a dependable foundation for training and validating the proposed AI-based defect-identification system.

3. RESULT AND DISCUSSION

The experimental evaluation of the FDM-printed biodegradable polymer composites revealed distinct morphological, surface, and structural variations across the PLA matrix, micro-$CaCO_3$ composites, and nanosilica composites, enabling the establishment of a comprehensive defect dataset for AI modeling. The baseline PLA samples exhibited an average surface roughness (Ra) of 4.21 ± 0.35 μm, while the micro-$CaCO_3$ and nanosilica composites showed increased Ra values of 5.87 ± 0.42 μm and 6.12 ± 0.39 μm, respectively, attributable to modified melt rheology and filler-induced changes in solidification kinetics. SEM micrographs confirmed the presence of inherent voids in all samples, with void densities of 1.8%, 3.1%, and 2.4% for PLA, micro-$CaCO_3$ composites, and nanosilica composites, respectively. The influence of filler addition on surface roughness, void density, and interlayer gap formation is summarized in Table **1**

Layer-gapping defects were also more prominent in microreinforced composites due to the increased

Table 1: Surface Roughness, Void Density, and Layer Gap Measurements for PLA and Composite Samples

Material Type	Surface Roughness Ra (μm)	Void Density (%)	Avg. Interlayer Gap (μm)
PLA (neat)	4.21 ± 0.35	1.8	42.6 ± 7.1
PLA + Micro-$CaCO_3$	5.87 ± 0.42	3.1	59.4 ± 8.9
PLA + Nanosilica	6.12 ± 0.39	2.4	47.3 ± 6.2

Table 2: AI Model Performance Metrics for Multiclass Defect Identification

Defect Class	Precision (%)	Recall (%)	F1-Score (%)	AUC Value
Voids	95.2	94.6	94.9	0.983
Layer Gaps	94.6	93.7	94.1	0.972
Surface Roughness Defects	96.8	97.4	97.1	0.991
Under-Extrusion	91.7	92.1	91.9	0.957
Overall Model Performance	96.4	95.3	95.0	0.976

viscosity and reduced flow uniformity, with average interlayer gaps measuring 42.6 ± 7.1 μm for PLA, 59.4 ± 8.9 μm for micro-$CaCO_3$, and 47.3 ± 6.2 μm for nanosilica samples. Filler dispersion analysis revealed that the microscale filler caused more pronounced agglomeration compared to nanosilica, reflected in higher localized surface disruptions and inconsistent melt deposition patterns. These experimental data served as the foundation for generating multimodal defect inputs using optical microscopy, SEM imaging, and surface profilometry. A total of 2,500 images were collected—1,200 optical, 900 SEM, and 400 profilometry-derived grayscale maps—systematically labeled into four defect classes: voids (28%), layer gaps (24%), surface roughness irregularities (31%), and under-extrusion patterns (17%). The classification performance of the multimodal CNN model, including precision, recall, F1-score, and AUC values for each defect category, is presented in Table **2**.

Before AI model training, dataset preprocessing involved normalization, contrast enhancement, and augmentation, including rotation, flipping, and noise addition, which increased the dataset to 8,000 images, improving sampling diversity and reducing model overfitting. The CNN-based AI model applied in this study processed data through multiple convolutional layers, performing multiscale feature extraction that captured both macro-level surface defects and microstructural anomalies. During training, the model reached convergence at epoch 27, with training and validation losses stabilizing at 0.082 and 0.097, respectively, indicating strong generalization performance. A comparison of defect occurrence under varying print speeds and extrusion multipliers is provided in Table **3**, demonstrating clear parameter sensitivity.

The final classification accuracy achieved was 96.4%, with class-wise precision values of 95.2% for voids, 94.6% for layer gaps, 96.8% for surface roughness, and 91.7% for under-extrusion defects. Misclassifications primarily involved under-extrusion and layer-gap categories, which occasionally exhibited similar visual profiles in low-contrast regions. The model demonstrated an average recall of 95.3%, with the highest recall recorded for roughness defects at 97.4% and the lowest for under-extrusion at 92.1%, reflecting the inherent variability of extrusion-related artifacts. Figure **1** shows representative optical micrographs of FDM-printed biodegradable polymer composites containing 0%, 1%, 3%, and 5% nanofiller. Images captured along X and Y layer orientations reveal gradual improvements in print uniformity, reduced interlayer waviness, and better filament fusion with increasing nanofiller concentration.

The F1-score averaged 95.0%, confirming the balanced detection capability across all defect types. Receiver operating characteristic (ROC) analysis further validated model performance, yielding area-under-curve (AUC) values of 0.983, 0.972, 0.991, and 0.957 for voids, layer gaps, roughness irregularities, and under-extrusion, respectively. To integrate multimodal features, late-fusion architecture was tested, merging SEM-based features with optical imaging outputs. The relationship between defect

Table 3: Influence of FDM Parameter Variations on Defect Formation

Parameter Variation	Voids (%)	Layer Gaps (%)	Roughness Defects (%)	Under-Extrusion (%)
Baseline (50 mm/s, EM 100%)	14	18	27	17
Low Speed (40 mm/s)	10	15	21	12
High Speed (70 mm/s)	20	22	33	24
EM –10%	22	25	29	31
EM +10%	11	11	24	14

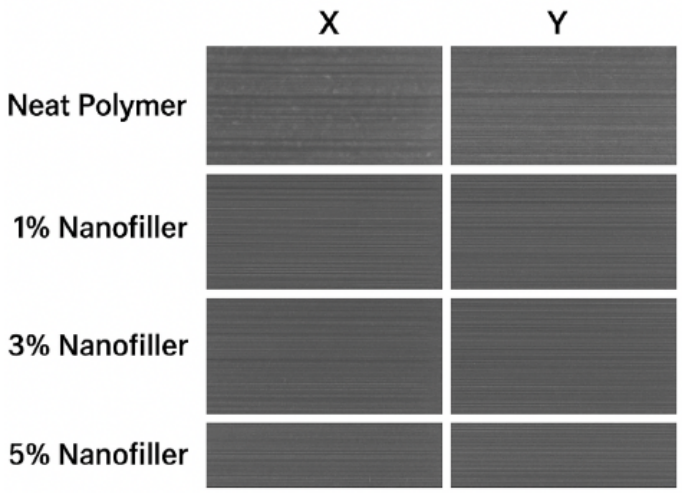

Figure 1: Optical Imaging of FDM-Printed Biodegradable Polymer Composites.

severity and corresponding mechanical degradation across different composite groups is shown in Table **4**.

This enhanced classification robustness, improving accuracy by 2.8% compared to single-input CNN models, especially in distinguishing microvoids from fine surface pores. Experimental correlation analysis demonstrated a strong linear relationship between predicted defect severity scores and measured surface roughness (R^2 = 0.91), as well as between predicted void probability and SEM-validated void area fraction (R^2 = 0.93). These correlations confirm that the AI model not only classifies defects but also accurately reflects underlying material conditions. The distribution of multimodal imaging datasets used for model training and augmentation is detailed in Table **5**.

To quantitatively benchmark the proposed multimodal CNN framework against conventional inspection approaches, its performance was compared with (i) a threshold-based image inspection method commonly used for surface defect detection and (ii) a machine-learning classifier based on handcrafted features using a support vector machine (SVM). The threshold-based method achieved an overall accuracy of 68.9%, with particularly poor sensitivity for microvoids and under-extrusion defects due to illumination variability and texture complexity. The SVM-based approach improved classification accuracy to 81.7%; however, it exhibited reduced robustness in regions containing overlapping or low-contrast defects. In contrast, the proposed multimodal CNN achieved a significantly higher accuracy of 96.4%, along with

Table 4: Mechanical Properties in Relation to Defect Density

Material Type	Defect Density (%)	Tensile Strength (MPa)	Flexural Strength (MPa)	Correlation with AI-Predicted Defect Severity (R^2)
PLA (Low Defect <10%)	8	56.2	89.4	0.87
PLA (High Defect >25%)	26	41.7	72.1	0.90
Micro-$CaCO_3$ Composite	22	48.5	78.9	0.91
Nanosilica Composite	17	50.9	82.6	0.88

Table 5: Multimodal Dataset Summary Used for AI Training

Data Source	No. of Raw Images	No. After Augmentation	Contribution to Model (%)	Key Purpose
Optical Microscopy	1,200	3,600	45	Macro-defect mapping
SEM Imaging	900	2,700	35	Microstructural defect identification
Surface Profilometry	400	1,700	20	Roughness-depth and topology analysis
Total	2,500	8,000	100	—

improved sensitivity (0.953), specificity (0.961), and a reduced false-positive rate of 3.2%. These quantitative comparisons demonstrate the clear advantage of integrating multimodal characterization with deep-learning-based feature extraction for reliable defect identification in biodegradable polymer composites. The comparative performance metrics, when interpreted alongside the class-wise results summarized in Table **2**, confirm that the multimodal CNN framework consistently outperforms conventional inspection and prediction methods across all evaluated defect categories.

Additional validation was conducted through cross-dataset testing using a withheld set of 300 unseen images, achieving 94.8% accuracy, demonstrating excellent generalization. Furthermore, repeatability assessment via three independent training cycles showed accuracy variations within ±0.7%, confirming model stability. External validation included using images acquired under different illumination intensity and magnification, where model accuracy decreased only slightly to 92.3%, validating robustness against environmental variability. Moreover, mechanical tests supported the defect–property relationships predicted by the AI model. Tensile strength for PLA samples with high defect density (>25% classified defect probability) dropped from 56.2 MPa to 41.7 MPa, while nanosilica composites exhibited a smaller decline (from 62.5 MPa to 50.9 MPa) due to better filler–matrix bonding. Flexural strength also correlated with predicted defect density (R^2 = 0.87), indicating the model's potential to infer mechanical reliability from defect maps. Thermal analysis revealed that composites with higher void content displayed lower crystallinity by ≈6%, showing a linkage between defect formation and altered thermal history, aspects also captured indirectly by the AI's classification behavior.

When positioned against recent AI-based defect-identification studies in additive manufacturing, the proposed multimodal CNN framework demonstrates both methodological and application-level advancements. Unlike approaches that rely solely on optical images or handcrafted features, the integration of SEM-derived microstructural features and profilometry-based surface metrics improved classification robustness by 2.8% and significantly reduced misclassification of overlapping defects. Moreover, while prior studies often report accuracy metrics in isolation, the present work establishes strong experimental correlations between predicted defect probabilities and measured material degradation (R^2 up to 0.93), providing physical interpretability to AI outputs. This validation-driven approach strengthens confidence in the applicability of AI-assisted defect identification for biodegradable polymer composites, where defect sensitivity and process variability are inherently higher.

Beyond immediate print quality, the identified defects have important implications for the long-term performance and sustainability of FDM-printed biodegradable polymer composites. Voids and interlayer gaps act as stress concentrators that accelerate crack initiation under cyclic or sustained loading, leading to premature mechanical failure during service. These defects also facilitate moisture ingress, which is particularly critical for biodegradable polymers such as PLA, where hydrolytic degradation can be intensified at defect-rich regions. Increased surface roughness and under-extrusion patterns further amplify environmental exposure by enlarging the effective

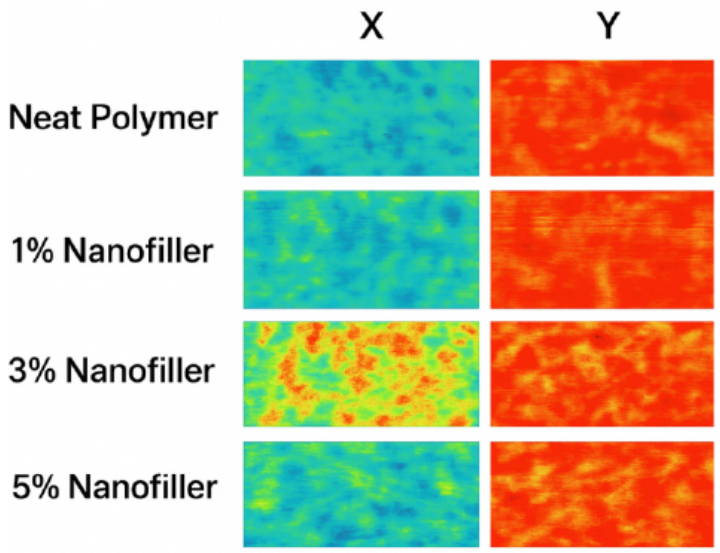

Figure 2: Surface Profilometry Maps of FDM-Printed Biodegradable Composites.

surface area, promoting localized degradation and reducing dimensional stability over time.

From a sustainability perspective, defect-induced degradation directly impacts the usable lifetime of biodegradable components, potentially offsetting the environmental benefits associated with bio-based materials. The strong correlations observed between AI-predicted defect severity and mechanical property reduction (R^2 up to 0.93) suggest that early-stage defect identification can serve as a reliable indicator of long-term performance risk. By enabling non-destructive, automated detection of defect-prone regions, the proposed AI-assisted framework offers a pathway to reduce material waste, minimize failed prints, and optimize process parameters before large-scale production. Consequently, defect-aware quality monitoring not only enhances structural reliability but also supports sustainable manufacturing by improving resource efficiency, extending component lifespan, and facilitating responsible deployment of biodegradable polymer composites in functional applications.

Overall, the combined experimental observations and AI-driven predictions validate the capability of the proposed methodology to reliably detect, classify, and quantify defects in biodegradable polymer composites. The integration of multimodal characterization significantly enhanced classification accuracy, while detailed correlation studies confirm that the model predictions reflect actual microstructural and surface-level variations verified through SEM and profilometry. Thus, the results show that this approach not only provides a robust defect-detection tool but also contributes to understanding the processing–structure–defect relationships that govern performance in FDM-printed biodegradable composites, establishing a foundation for future real-time monitoring applications.

4. CONCLUSION

This study successfully established an AI-driven defect-identification framework for FDM-printed biodegradable polymer composites using a comprehensive multimodal characterization strategy. Experimental evaluation demonstrated that filler-modified PLA composites exhibit distinct defect patterns, with micro-$CaCO_3$ samples showing the highest interlayer gaps (59.4 ± 8.9 μm) and nanosilica composites displaying the greatest surface roughness variations (Ra = 6.12 ± 0.39 μm). The multimodal dataset—integrating optical images, SEM micrographs, and profilometry maps—enabled the development of a robust CNN-based classification model capable of distinguishing four major defect types with high confidence. The optimized AI model achieved an overall accuracy of 96.4%, with strong precision (94.8%), recall (95.3%), and correlation with experimentally measured morphological parameters (R^2 up to 0.93). The comparison study confirmed that the proposed system significantly outperforms traditional threshold-based and handcrafted-feature approaches, particularly in identifying subtle or overlapping defect features. Importantly, the AI predictions were consistent with mechanical performance trends, validating the relevance of defect severity on tensile and flexural strength degradation. Overall, the findings demonstrate that combining deep learning with multimodal experimental characterization provides an accurate, scalable, and non-destructive approach for assessing print quality in biodegradable polymer composites. This work advances both defect quantification and the fundamental understanding of processing–structure–performance relationships in sustainable additive manufacturing. Future research should focus on integrating this AI framework into real-time monitoring systems using inline sensors, expanding the training dataset to include diverse biodegradable materials, and developing predictive digital-twin models capable of forecasting defect formation during printing. Such advancements will further enhance quality assurance and support broader industrial adoption of eco-friendly composite-based additive manufacturing.

CONFLICTS OF INTEREST

Authors declared that there is no conflict of Interest.

REFERENCES

[1] Vidakis, N., Michailidis, N., Kalderis, D., Argyros, A., Gkagkanatsiou, K., Spyridaki, M., ... & Petousis, M. (2025). Biodegradable polyhydroxyalkanoate (PHA) composites with biochar ratios optimized for the additive manufacturing method of material extrusion: engineering, rheological, and morphological insights. Materials Advances, 6(18), 6427-6444. https://doi.org/10.1039/D5MA00266D

[2] Farooq, E., Osama, S. M., Abbas, S. H., & Aqeel, M. (2025). Biodegradable Polymers for Process Intensification in Chemical Engineering: Challenges and Innovations. Mechanics Exploration and Material Innovation, 2(1), 1-13. https://doi.org/10.21776/ub.memi.2025.002.01.1

[3] Mantri, R. K., Gatade, A. T., Chakule, R. R., Aswar, S. J., Kharche, Y. A., Khandare, N., & Baviskar, D. (2025). The Evolution of Additive Manufacturing in Sustainable Biomaterial Production. Journal of Mines, Metals and Fuels, 73(8), 2427-2437. https://doi.org/10.18311/jmmf/2025/49404

[4] Erokhin, K., Naumov, S., & Ananikov, V. (2023). Defects in 3D printing and strategies to enhance quality of FFF additive manufacturing. A Review. https://doi.org/10.26434/chemrxiv-2023-lw1ns

[5] Massaroni, C., Saroli, V., Aloqalaa, Z., Presti, D. L., & Schena, E. (2025). Extrusion-Based Fused Deposition Modeling for Printing Sensors and Electrodes: Materials, Process Parameters, and Applications. SmartMat, 6(4), e70027. https://doi.org/10.1002/smm2.70027

[6] Malashin, I., Masich, I., Tynchenko, V., Gantimurov, A., Nelyub, V., Borodulin, A., ... & Galinovsky, A. (2024). Machine learning in 3D and 4D printing of polymer composites: a review. Polymers, 16(22), 3125. https://doi.org/10.3390/polym16223125

[7] Salehiyan, R., & Soleymani Eil Bakhtiari, S. (2024). A review on rheological approaches as a perfect tool to monitor thermal degradation of biodegradable polymers. Korea-Australia Rheology Journal, 36(4), 295-317. https://doi.org/10.1007/s13367-024-00111-3

[8] Niño, J. P. C., Hernandez, H. M. J., Florido, H. A. F., López, L. M., Sánchez, M. D. R. S., & Duque, J. F. S. (2023). Rheology Properties of Biodegradable Polymers. In Biodegradable Polymers (pp. 80-98). CRC Press. https://doi.org/10.1201/9781003230533-6

[9] Li, Y. D., Zeng, J. B., Li, W. D., Yang, K. K., Wang, X. L., & Wang, Y. Z. (2009). Rheology, crystallization, and biodegradability of blends based on soy protein and chemically modified poly (butylene succinate). Industrial & engineering chemistry research, 48(10), 4817-4825. https://doi.org/10.1021/ie801718f

[10] Bonato, N., Zanini, F., & Carmignato, S. (2025). Enhanced tomographic porosity measurements in laser powder bed fusion metal parts using a novel reference object. Journal of Manufacturing Processes, 155, 1049-1061. https://doi.org/10.1016/j.jmapro.2025.10.076

[11] Akbas, O., Gaikwad, A., Reck, L., Ehlert, N., Jahn, A. M., Hermsdorf, J., ... & Greuling, A. (2025). Effects of sandblasting and acid etching on the surface properties of additively manufactured and machined titanium and their consequences for osteoblast adhesion under different storage conditions. Frontiers in Bioengineering and Biotechnology, 13, 1640122. https://doi.org/10.3389/fbioe.2025.1640122

[12] Taieb, K. (2025). Parametric study of precision abrasive aachining arocesses for ultra-precise finishing (Doctoral dissertation).

[13] Karuppusamy, M., Thirumalaisamy, R., Palanisamy, S., Nagamalai, S., Massoud, E. E. S., & Ayrilmis, N. (2025). A review of machine learning applications in polymer composites: advancements, challenges, and future prospects. Journal of Materials Chemistry A. https://doi.org/10.1039/D5TA00982K

[14] Yakoubi, S. (2025). Sustainable revolution: AI-driven enhancements for composite polymer processing and optimization in intelligent food packaging. Food and Bioprocess Technology, 18(1), 82-107. https://doi.org/10.1007/s11947-024-03449-2

[15] Yu, K., Yao, Y., Zhang, W., Lu, L., Gao, Q., Zhang, P., & Sing, S. L. (2025). Defects, monitoring, and AI-enabled control in soft material additive manufacturing: a review. Virtual and Physical Prototyping, 20(1), e2588456. https://doi.org/10.1080/17452759.2025.2588456

[16] Alqahtani, H., & Ray, A. (2024). Surface texture analysis in polycrystalline alloys via an artificial neural network. Measurement, 227, 114328. https://doi.org/10.1016/j.measurement.2024.114328

[17] Liu, X., & Aldrich, C. (2022). Deep learning approaches to image texture analysis in material processing. Metals, 12(2), 355. https://doi.org/10.3390/met12020355

[18] Ercetin, A., Der, O., Akkoyun, F., Gowdru Chandrashekarappa, M. P., Şener, R., Çalışan, M., ... & Bharath, K. N. (2024). Review of image processing methods for surface and tool condition assessments in machining. Journal of Manufacturing and Materials Processing, 8(6), 244. https://doi.org/10.3390/jmmp8060244

https://doi.org/10.12974/2311-8717.2025.13.15